

An L-DEIM Induced High Order Tensor Interpolatory Decomposition

Zhengbang Cao*

Yimin Wei[†]Pengpeng Xie[‡]

Abstract

This paper derives the CUR-type factorization for tensors in the Tucker format based on a new variant of the discrete empirical interpolation method known as L-DEIM. This novel sampling technique allows us to construct an efficient algorithm for computing the structure-preserving decomposition, which significantly reduces the computational cost. For large-scale datasets, we incorporate the random sampling technique with the L-DEIM procedure to further improve efficiency. Moreover, we propose randomized algorithms for computing a hybrid decomposition, which yield interpretable factorization and provide a smaller approximation error than the tensor CUR factorization. We provide comprehensive analysis of probabilistic errors associated with our proposed algorithms, and present numerical results that demonstrate the effectiveness of our methods.

Keywords: CUR decomposition; L-DEIM; low-rank approximation; Tucker decomposition; randomized algorithm

Mathematics Subject Classification: 15A23, 15A69

1 Introduction

Tensor decompositions [8, 19, 31, 32, 36, 42], are efficient and widely used for multi-way data processing, and in particular, they can be utilized to compress the data tensors without destroying their intrinsic multidimensional structure. This work presents new algorithms for computing the CUR-type and hybrid CUR-type factorizations for tensors in the Tucker format based on a novel index selection procedure, that is, the L-discrete empirical interpolation method (L-DEIM) [23]. Further, random sampling techniques [27, 34] are also utilized to enhance the efficiency of the proposed algorithms.

A CUR factorization [21, 28, 40] is a low-rank approximation of a matrix $X \in \mathbb{R}^{m \times n}$ of the form

$$X \approx CUR, \quad (1.1)$$

where C and R are the matrices that consist of actual columns and rows of A , inheriting certain important properties of the original matrix, such as sparsity, non-negativity, integer-values and so on. This novel property has rendered the CUR a potent tool for data analysis and attractive in a wide range of applications. To deal with the multi-dimensional data, the CUR-type decomposition for tensors was proposed by [16, 18, 20], and the perturbation analysis and sampling strategy were also

*School of Mathematical Sciences, Ocean University of China, Qingdao 266100, China. E-Mail: caozhengbang@stu.ouc.edu.cn

[†]School of Mathematical Sciences and Key Laboratory of Mathematics for Nonlinear Sciences, Fudan University, Shanghai 200433, China. E-Mail: ymwei@fudan.edu.cn

[‡]Corresponding author (P. Xie). School of Mathematical Sciences, Ocean University of China, Qingdao 266100, China. E-Mail: xie@ouc.edu.cn.

researched in [2, 7, 10]. For tensors in the Tucker format, [20] provides a multilinear rank- (r_1, r_2, \dots, r_d) approximation for a given tensor $\mathcal{X} \in \mathbb{R}^{I_1 \times I_2 \times \dots \times I_d}$ such that

$$\mathcal{X} \approx \mathcal{G} \times_1 C_1 \times_2 C_2 \times \dots \times_d C_d, \quad (1.2)$$

where $\mathcal{G} \in \mathbb{R}^{r_1 \times r_2 \times \dots \times r_d}$ is a core tensor, and the columns of matrices $\{C_n\}_{n=1}^d \in \mathbb{R}^{I_n \times r_n}$ are generated by sampling from the mode- n fibers of \mathcal{X} , using a probability distribution that is dependent on the norms of the columns. The author in [37] derived a factorization of the form (1.2) based on the interpolatory decomposition [17, 43], which was denoted as higher order interpolatory decomposition (HOID), where a number of sophisticated techniques for subset selection, including the DEIM [5, 9], leverage score sampling [30, 33], strong rank-revealing QR (RRQR) [26] and QR decomposition with column pivoting (PQR) [22] were also extended to the domain of tensors. Numerical examples in [37] demonstrate that the accuracy of the approximation heavily relies on the sampling technique utilized. Results show that the DEIM method incurs errors that are comparable to those of the strong RRQR method, while outperforming the leverage score approach. Nevertheless, it should be noted that the DEIM approach demands the computation of the singular value decomposition (SVD) for each mode, and the number of indices that can be chosen is limited by the number of input singular vectors. These characteristics make it challenging to apply DEIM in the context of big data problems, where the computation of singular vectors of tensor unfolding can prove to be a formidable task.

In recent times, a novel variant of the DEIM named L-DEIM has been introduced [23]. This new method embodies a hybrid approach that leverages the advantageous properties of both deterministic leverage scores and DEIM, allowing for the selection of a larger number of indices than input singular vectors, while still achieving outcomes that are comparable to those of the original DEIM. In this paper, leveraging this novel sampling procedure, we develop efficient algorithms for computing a multilinear rank- (r_1, r_2, \dots, r_d) approximation of the form (1.2). To be specific, during the process of constructing the approximation, the L-DEIM procedure operates on the \hat{r}_n right singular vectors of the mode- n unfolding to select the indices, where $\hat{r}_n \leq r_n$, and in practice, a value of $\hat{r}_n = r_n/2$ has been found to yield favorable empirical results, just as shown in [23]. Consequently, our proposed algorithm is especially advantageous in the scenarios involving large-scale data, where computing the r_n singular value vectors of mode- n unfolding is computationally expensive even for moderately small values of r_n . Despite its benefits, computationally, the L-DEIM induced HOID still necessitates the input of the SVD of each tensor unfolding, which can be prohibitively expensive for the tensors with large dimensions d or for those with significant storage requirements. Inspired by the remarkable achievements of randomized algorithms explored in [1, 11–15, 35], we incorporate random sampling techniques into our algorithm to enhance its efficiency, which facilitates matrix and tensor decompositions by not only decreasing the computational complexity of deterministic algorithms, but also reducing inter-level memory communication. Specifically, there are two distinct computational stages involving the processing of generating the factor matrices $\{C_n\}_{n=1}^d$. In the first stage, we leverage random sampling methods [34] to perform a mode-wise reduction of the unfolding matrices. This enables the construction of a low-dimensional subspace that faithfully captures the essential actions of the unfolding matrices. Subsequently, in the second stage, we implement the L-DEIM procedure to operate on the singular matrices approximated in the first stage. The aim of this procedure is to selectively sample the fibers, which constitute a pivotal component of the factorization process. In certain applications, it may be advisable to selectively sample fibers in only certain modes, rather than all of them. In such cases, a hybrid CUR-type Tucker decomposition, as proposed in [6], is preferred over the factorization (1.2), since it provides a smaller approximation error. By combining the randomized techniques and the sampling procedures such as the PQR, DEIM and L-DEIM, we provide three versions of efficient randomized algorithms for computing a hybrid CUR-type Tucker decomposition. Compared with the CUR-type and hybrid CUR-type Tucker decomposition algorithms based on the regular sampling procedure such as the PQR, RRQR and DEIM, our algorithms allow for a comparable accuracy with significantly lower cost and will be more computationally efficient

on large-scale data. Details of the algorithm and theoretical analysis with the numerical results are provided to demonstrate the effectiveness of our approaches.

The rest of this article is organized as follows. In Section 2, we introduce some basic notation and describe several sampling techniques including the DEIM, the deterministic leverage score and the L-DEIM. Then we review some existing tensor decomposition, notably the higher order singular value decomposition (HOSVD) [32], the HOID and the hybrid decomposition. Next, in Section 3 we present our algorithm for computing the HOID based on the Tucker factorization using the L-DEIM procedure, where the error bound is also presented in detail. In Section 4, we develop randomized algorithms for computing the HOID based on the sampling procedure L-DEIM, along with detailed probabilistic error analysis. The special cases where the dimensions of the input tensors are restricted to dimension 2, i.e., matrices are also considered. In Section 5, we provide new randomized algorithms for computing the hybrid decomposition and derive the probabilistic error analysis of the proposed algorithms. In Section 6, we test the performance of the proposed algorithms on several synthetic tensors and real-world datasets. Finally, in Section 7, we end this paper with concluding remarks.

2 Preliminaries

2.1 Background on tensors

We begin by introducing fundamental notation and concepts for tensors. For a more comprehensive treatment, we refer readers to [32]. A d -dimensional tensor is represented by $\mathcal{X} \in \mathbb{R}^{I_1 \times I_2 \times \dots \times I_d}$ where the entries of \mathcal{X} are denoted by

$$x_{j_1 j_2 \dots j_d}, \quad 1 \leq j_1 \leq I_1, 1 \leq j_2 \leq I_2, \dots, 1 \leq j_d \leq I_d.$$

The norm of a d -dimensional tensor \mathcal{X} with entries $x_{j_1 j_2 \dots j_d}$ is defined by

$$\|\mathcal{X}\|_F = \sqrt{\sum_{j_1=1}^{I_1} \sum_{j_2=1}^{I_2} \dots \sum_{j_d=1}^{I_d} |x_{j_1 j_2 \dots j_d}|^2}.$$

The vector 2-norm and the matrix norm it induces are denoted by $\|\cdot\|$. $X_{(n)} \in \mathbb{R}^{I_n \times \prod_{k \neq n} I_k}$ represents the n th mode unfolding of the tensor \mathcal{X} . The multilinear rank of \mathcal{X} is a tuple (r_1, r_2, \dots, r_d) where r_n is the rank of $X_{(n)}$. The n -mode product of the tensor \mathcal{X} with a matrix $U \in \mathbb{R}^{k \times I_n}$ is represented $\mathcal{X} \times_n U$, generating a tensor $\mathcal{Y} \in \mathbb{R}^{I_1 \times \dots \times I_{n-1} \times k \times I_{n+1} \times \dots \times I_d}$, and elementwise,

$$y_{i_1 \dots i_{n-1} i i_{n+1} \dots i_d} = \sum_{i_n=1}^{I_n} x_{i_1 \dots i_d} u_{i i_n}.$$

It can also be expressed in terms of matrix unfolding:

$$\mathcal{Y} = \mathcal{X} \times_n U \quad \Leftrightarrow \quad Y_{(n)} = U X_{(n)}.$$

For a series of multiplications involving distinct modes, the following relationships hold:

$$\mathcal{X} \times_m Y \times_n Z = \mathcal{X} \times_n Z \times_m Y \quad (m \neq n), \quad \mathcal{X} \times_n Y \times_n Z = \mathcal{X} \times_n (ZY). \quad (2.1)$$

To index vectors and matrices, we use MATLAB notation throughout this paper. For example, $X(\mathbf{q}, :)$ represents the k rows of X indexed by the indices set $\mathbf{q} \in \mathbb{N}^k$.

Now we are set to introduce several algorithms that produce a multilinear rank- (r_1, r_2, \dots, r_d) approximation to tensors in the Tucker format, i.e., the HOSVD, HOID and the hybrid algorithm.

Given a tensor $\mathcal{X} \in \mathbb{R}^{I_1 \times I_2 \times \dots \times I_d}$, the HOSVD algorithm computes a core tensor $\mathcal{U} \in \mathbb{R}^{r_1 \times r_2 \times \dots \times r_d}$ and a collection of matrices $U_j \in \mathbb{R}^{I_j \times r_j}$ containing the r_j leading left singular vectors of $X_{(n)}$, $n = 1, 2, \dots, d$ such that

$$\mathcal{X} \approx \mathcal{U} \times_1 U_1 \times_2 U_2 \times \dots \times_d U_d. \quad (2.2)$$

Although the approximation error obtained by (2.2) is theoretically smaller than that of (1.2), the CUR-type approximation facilitates interpreting the underlying data tensors and decomposing tensors so that their structures can be potentially preserved. For certain applications where it may be appropriate to sample fibers in only some of the modes, rather than all of them, the author in [6] proposed a hybrid CUR-type decomposition, which provides a decomposition such that

$$\mathcal{X} \approx \mathcal{G} \times_1 C_1 \cdots \times_t C_t \times_{t+1} U_{t+1} \cdots \times_d U_d, \quad (2.3)$$

where $\mathcal{G} \in \mathbb{R}^{r_1 \times r_2 \times \dots \times r_d}$ is a core tensor, and the columns of matrices $\{C_i\}_{i=1}^t \in \mathbb{R}^{I_i \times r_i}$ are extracted from the mode- i fibers of \mathcal{X} , while orthonormal matrices $\{U_j\}_{j=t+1}^d \in \mathbb{R}^{I_j \times r_j}$ are selected to minimize the approximation error. Consequently, the approximation error obtained this way is smaller than the one from (1.2).

2.2 Subset selection procedure

We now give a concise introduction to several subset selection procedures.

Assume the best rank- k SVD of $X \approx V \Sigma W^T$ is available, where matrices V and W consist of the k leading left and right singular vectors of X respectively. The deterministic leverage score sampling algorithm extracts k columns of X corresponding to the indices of the largest leverage scores $\ell_i = \|W(i, :)\|^2$. While the simplicity of this approach has yielded remarkable success in practical applications, we note that a complete theoretical guarantee has yet to be established.

The DEIM [9] is an index selection procedure that gives simple, deterministic CUR factorizations for both matrices and tensors. The authors in [40] and [37] utilized this procedure in the context of subset selection to CUR factorization for matrices and tensors respectively. Specifically, the DEIM algorithm follows a sequential procedure to process the columns of matrices V and W , beginning with the first dominant singular vector, and the next index corresponds to the largest magnitude in the residual vector. See the pseudocode in Algorithm 1 for more details.

Algorithm 1 DEIM index selection [9]

Require: $V \in \mathbb{R}^{m \times k}$, $W \in \mathbb{R}^{n \times k}$ with $k \leq \min(m, n)$.

- 1: $v = V(:, 1)$.
 - 2: $p_1 = \operatorname{argmax}_{1 \leq i \leq n} |v_i|$.
 - 3: $\mathbf{p} = [p_1]$.
 - 4: **for** $j = 2, 3, \dots, k$ **do**
 - 5: $v = V(:, j)$.
 - 6: $r = v - V(:, 1:j-1)(V(\mathbf{p}, 1:j-1) \setminus v(\mathbf{p}))$.
 - 7: $p_j = \operatorname{argmax}_{1 \leq i \leq m} |r_i|$.
 - 8: $\mathbf{p} = [\mathbf{p} \ p_j]$.
 - 9: **end for**
 - 10: Perform 1-9 on W to obtain the index \mathbf{q} .
 - 11: **return** column and row index $\mathbf{q}, \mathbf{p} \in \mathbb{N}_+^k$ respectively, with non-repeating entries.
-

However, a major limitation of DEIM is its inability to select indices beyond the number of available singular vectors. To overcome this shortcoming, a novel variant of DEIM, called L-DEIM (Algorithm 2), which integrates the advantage of leverage score sampling and the DEIM procedures,

was proposed in [23]. There are two principal steps involved in this method. Firstly, the standard DEIM procedure is executed to select the initial \hat{k} indices. Subsequently, the 2-norm of the rows of the residual singular vectors is computed to select the additional $k - \hat{k}$ indices. By adopting this method, only \hat{k} singular vectors are required to obtain k indices. It is concluded in [23] that L-DEIM is computationally more efficient than the original DEIM, while the accuracy of both methods can be comparable if the parameter \hat{k} is chosen appropriately. Besides, the L-DEIM algorithm degenerates to the DEIM algorithm, if we set $\hat{k} = k$.

Algorithm 2 L-DEIM index selection [23]

Require: $V \in \mathbb{R}^{m \times \hat{k}}$ and $W \in \mathbb{R}^{n \times \hat{k}}$, target rank k with $\hat{k} \leq k \leq \min(m, n)$.

- 1: **for** $j = 1, 2, \dots, \hat{k}$ **do**
- 2: $\mathbf{p}(j) = \operatorname{argmax}_{1 \leq i \leq m} |(V(i, j))|$.
- 3: $V(:, j+1) = V(:, j+1) - V(:, 1:j) \cdot (V(\mathbf{p}, 1:j) \setminus V(\mathbf{p}, j+1))$.
- 4: **end for**
- 5: Compute $\ell_i = \|V(i, :)\|$ for $i = 1, 2, \dots, m$.
- 6: Sort ℓ in non-increasing order.
- 7: Remove entries in ℓ corresponding to the indices in \mathbf{p} .
- 8: $\mathbf{p}' = k - \hat{k}$ indices corresponding to $k - \hat{k}$ largest entries of ℓ .
- 9: $\mathbf{p} = [\mathbf{p}; \mathbf{p}']$.
- 10: Perform 1-9 on W to get index set \mathbf{q} .
- 11: **return** column and row indices $\mathbf{q}, \mathbf{p} \in \mathbb{N}_+^k$ respectively, with non-repeating entries.

3 L-DEIM based HOID

This section derives a new variant of the HOID algorithm for representing low multilinear rank tensors $\mathcal{X} \in \mathbb{R}^{I_1 \times I_2 \times \dots \times I_d}$ of the form (1.2) based on the L-DEIM procedure.

As mentioned earlier, the factor matrices $\{C_n\}_{n=1}^d$ of (1.2) are formed by extracting r_n columns from the mode- n tensor unfolding $X_{(n)}$, where the index sets of the selected columns are denoted by \mathbf{s} . We assume that the best rank- \hat{r}_n SVD $X_{(n)} \approx V_n \Sigma W_n^T$, $\hat{r}_n \leq r_n$ are available. Then we compute \mathbf{s} by applying the L-DEIM algorithm on the matrix W_n . Once $\{C_n\}_{n=1}^d$ are obtained, the core tensor is computed as

$$\mathcal{G} = \mathcal{X} \times_1 C_1^\dagger \times_2 C_2^\dagger \cdots \times_d C_d^\dagger, \quad (3.1)$$

which is optimal in the Frobenius norm [40], where C_i^\dagger is the Moore-Penrose inverse of C_i [44].

We introduce our L-DEIM based HOID algorithm in Algorithm 3. As stated in [37], for certain applications, it is often unnecessary to compute the core tensor \mathcal{G} . Utilizing the novel subset selection algorithm L-DEIM, our proposed algorithm allows to form a multilinear rank- (r_1, r_2, \dots, r_d) approximation for the given tensor \mathcal{X} without having to compute r_n right singular vectors of mode- n tensor unfolding $X_{(n)}$, $n = 1, 2, \dots, d$ and it only requires a smaller \hat{r}_n instead. Hence, the new method is particularly appealing in the cases where computing the singular vectors is computationally expensive and the dimension d is prohibitively large.

We now derive an estimate for the error incurred to produce a HOID based on the L-DEIM. Before that, we first present a result related to [37, Lemma 2.1].

Lemma 3.1. *Let the factor matrices $C_n, n = 1, 2, \dots, d$ and the core tensor \mathcal{G} be computed as in (3.1),*

Algorithm 3 L-DEIM based HOID

Require: $\mathcal{X} \in \mathbb{R}^{I_1 \times I_2 \times \dots \times I_d}$, desired multilinear rank (r_1, r_2, \dots, r_d) and parameter $(\hat{r}_1, \hat{r}_2, \dots, \hat{r}_d)$.

- 1: **for** $n = 1, 2, \dots, d$ **do**
- 2: Compute \hat{r}_n right singular vectors $W_n \in \mathbb{R}^{\prod_{k \neq n} I_k \times \hat{r}_n}$ of mode- n tensor unfolding $X_{(n)}$.
- 3: **for** $j = 1, 2, \dots, \hat{r}_n$ **do**
- 4: $\mathbf{s}(j) = \operatorname{argmax}_{1 \leq i \leq \prod_{k \neq n} I_k} |(W_n(i, j))|$.
- 5: $W_n(:, j+1) = W_n(:, j+1) - W_n(:, 1:j) \cdot (W_n(\mathbf{s}, 1:j) \backslash W_n(\mathbf{s}, j+1))$.
- 6: **end for**
- 7: Compute $\ell_i = \|W_n(i, :)\|$ for $i = 1, 2, \dots, \prod_{k \neq n} I_k$.
- 8: Sort ℓ in non-increasing order.
- 9: Remove entries in ℓ corresponding to the indices in \mathbf{s} .
- 10: $\mathbf{s}' = r_n - \hat{r}_n$ indices corresponding to $r_n - \hat{r}_n$ largest entries of ℓ .
- 11: $\mathbf{s} = [\mathbf{s}; \mathbf{s}']$.
- 12: Form $C_n = X_{(n)}(:, \mathbf{s})$.
- 13: **end for**
- 14: Compute core tensor $\mathcal{G} \in \mathbb{R}^{r_1 \times r_2 \times \dots \times r_d}$ as $\mathcal{G} = \mathcal{X} \times_1 C_1^\dagger \times_2 C_2^\dagger \dots \times_d C_d^\dagger$.
- 15: **return** Tucker decomposition $\mathcal{X} \approx \mathcal{G} \times_1 C_1 \times_2 C_2 \dots \times_d C_d$.

then we have the following error bound

$$\|\mathcal{X} - \mathcal{G} \times_1 C_1 \times_2 C_2 \dots \times_d C_d\|_F^2 \leq \sum_{n=1}^d \left\{ \min(I_n, \prod_{k \neq n} I_k) \left\| (I - C_n C_n^\dagger) X_{(n)} \right\|_F^2 \right\}.$$

Proof. By the definition of core tensor \mathcal{G} and the property (2.1), we have

$$\mathcal{G} \times_1 C_1 \times_2 C_2 \dots \times_d C_d = \mathcal{X} \times_1 (C_1 C_1^\dagger) \times_2 \dots \times_d (C_d C_d^\dagger).$$

Recalling the result in [37, Lemma 2.1], for orthogonal projections $\{\Pi_i\}_{i=1}^n$, we have

$$\|\mathcal{X} - \mathcal{X} \times_1 \Pi_1 \times_2 \Pi_2 \dots \times_d \Pi_d\|_F^2 \leq \sum_{n=1}^d \|\mathcal{X} - \mathcal{X} \times_n \Pi_n\|_F^2.$$

Observe that $C_n C_n^\dagger$ is an orthogonal projection matrix, it follows that

$$\begin{aligned} \|\mathcal{X} - \mathcal{G} \times_1 C_1 \times_2 C_2 \dots \times_d C_d\|_F^2 &= \|\mathcal{X} - \mathcal{X} \times_1 (C_1 C_1^\dagger) \dots \times_d (C_d C_d^\dagger)\|_F^2 \\ &\leq \sum_{n=1}^d \|\mathcal{X} - \mathcal{X} \times_n (C_n C_n^\dagger)\|_F^2 \\ &\leq \sum_{n=1}^d \|(I - C_n C_n^\dagger) X_{(n)}\|_F^2 \\ &\leq \sum_{n=1}^d \left\{ \min(I_n, \prod_{k \neq n} I_k) \left\| (I - C_n C_n^\dagger) X_{(n)} \right\|_F^2 \right\}. \end{aligned}$$

□

The following theorem quantifies the error of the HOID produced by Algorithm 3.

Theorem 3.1. Suppose that $\mathcal{X} \in \mathbb{R}^{I_1 \times I_2 \times \dots \times I_d}$ with $I_n \leq \prod_{k \neq n} I_k$ for $n = 1, 2, \dots, d$. Let the matrices C_n for $n = 1, 2, \dots, d$ and the core tensor \mathcal{G} be computed according to Algorithm 3. Then we have the following error bound

$$\|\mathcal{X} - \mathcal{G} \times_1 C_1 \times_2 C_2 \cdots \times_d C_d\|_F^2 \leq \sum_{n=1}^d \left[I_n \left(\prod_{k \neq n} I_k \right) \frac{4^{\hat{r}_n} \cdot \hat{r}_n}{3} \right] \sigma_{\hat{r}_n+1}^2,$$

where $\sigma_{\hat{r}_n+1}$ is the $(\hat{r}_n + 1)$ th largest singular value of the mode- n tensor unfolding $X_{(n)}$.

Proof. It follows from Lemma 3.1 that

$$\|\mathcal{X} - \mathcal{G} \times_1 C_1 \times_2 C_2 \cdots \times_d C_d\|_F^2 \leq \sum_{n=1}^d \left\{ I_n \|(I - C_n C_n^\dagger) X_{(n)}\|^2 \right\}.$$

Let \mathbf{s} be the indices obtained by performing the L-DEIM to the right singular matrices W_n of $X_{(n)}$ and set $S = I(:, \mathbf{s})$. Denote the interpolatory projectors $\mathbb{S} = S(W_n^T S)^\dagger W_n$. Combining the result in [29, Lemma 3] that $\|(I - C_n C_n^\dagger) X_{(n)}\| \leq \|X_{(n)}(I - \mathbb{S})\|$ with [29, Lemma 2], we have

$$\begin{aligned} \|(I - C_n C_n^\dagger) X_{(n)}\| &\leq \|X_{(n)}(I - \mathbb{S})\| = \|X_{(n)}(I - W_n W_n^T)(I - \mathbb{S})\| \\ &\leq \|X_{(n)}(I - W_n W_n^T)\| \|I - \mathbb{S}\| = \|I - \mathbb{S}\| \sigma_{\hat{r}_n+1} \\ &= \|(W_n^T S)^\dagger\|, \end{aligned}$$

where we use the fact that $\|I - \mathbb{S}\| = \|\mathbb{S}\| = \|(W_n^T S)^\dagger\|$ for $\mathbb{S} \neq 0$ or I [41]. Applying the result in [24] that $\|(W_n^T S)^\dagger\| \leq \sqrt{\frac{\hat{r}_n \cdot \prod_{k \neq n} I_k}{3}} 2^{\hat{r}_n}$, we obtain the desired result. \square

4 Randomization for HOID

During the process of the DEIM and L-DEIM based HOID, the main cost lies in calculating the singular vectors of each mode tensor unfolding. When dealing with large-scale problems, the leading singular vectors can be effectively computed using the randomized algorithms [14, 34]. Motivated by this success, in this section, utilizing the random sampling methods [34], we develop the randomized algorithms for computing the HOID based on the two sampling procedures. Moreover, we consider the scenario where the dimension of the input tensor is constrained to dimension 2, that is, matrices and provide a fast randomized algorithm for matrix CUR decomposition.

4.1 Randomization for DEIM based HOID

The computation of the complete SVD of a matrix $X \in \mathbb{R}^{m \times n}$ costs $\mathcal{O}(nm^2)$, assuming $n \geq m$. However, this computational expense can be prohibitively high when the dimensions are large. The randomized SVD algorithm, developed in [34], provides a simple and efficient technique for generating an accurate approximation of the SVD for a given matrix, which comprise two distinct stages.

During the first stage, we multiply X by a Gaussian random matrix with entries having zero mean and unit variance. This results in a set of random linear combinations of the rows of X . Subsequently, we construct a matrix Q that approximates the range of X , thereby yielding the approximation $X \approx XQQ^T$. In the second stage, we compute a thin SVD of the much smaller matrix $XQ = V\Sigma U^T$. We then truncate the decomposition to the desired rank, and compute $W = QU$ to obtain the

approximated right singular matrices. The operations yield the rank- r approximation $X \approx XQQ^T = V\Sigma W^T$, and the error bound

$$\|V\Sigma W^T - X\| \leq \left(2\sqrt{2(r+p)m\beta^2\gamma^2 + 1} + 2\sqrt{2(r+p)m\beta\gamma}\right) \sigma_{r+1} \quad (4.1)$$

holds with probability not less than

$$\chi = 1 - \frac{1}{\sqrt{2\pi(l-r+1)}} \left(\frac{e}{(l-r+1)\beta}\right)^{l-r+1} - \frac{1}{2(\gamma^2-1)\sqrt{\pi m\gamma^2}} \left(\frac{2\gamma^2}{e^{\gamma^2-1}}\right)^m, \quad (4.2)$$

where σ_{r+1} is the $(r+1)$ th largest singular value of X , l is a user-specified integer with $l = r + p$, and p is the oversampling parameter utilized to augment the number of columns in order to enhance the flexibility of the computational method, β and γ are positive real numbers such that $\gamma > 1$. To illustrate the use of these parameters, we choose $\beta = 3/4$, $\gamma^2 = 5$, and $p = 20$. With this choice, we can derive the above error bound, which holds with probability not less than $1 - 10^{-17}$. [34, Table 1] presents similar results obtained by varying the values of l , β , and γ .

We summarize our randomized approach in Algorithm 4, where we obtain an approximation $\hat{\mathcal{X}}$ of given tensor \mathcal{X} in a CUR-type Tucker format

$$\hat{\mathcal{X}} = \mathcal{G} \times_1 C_1 \times_2 C_2 \cdots \times_d C_d.$$

In Algorithm 4, we leverage the randomization techniques in [34] to expedite the SVD process and acquire the singular vectors of mode tensor unfolding $X_{(n)}$ for $n = 1, 2, \dots, d$. Next, we exploit the DEIM index selection procedure, operating on the approximate singular vector matrices to identify the selection fibers and construct matrices $\{C_n\}_{n=1}^d$. Compared to the randomized approach proposed in [37], which performs well in numerical results, however, without a complete error analysis, we establish a detailed probabilistic error analysis for our randomized algorithm.

Algorithm 4 Randomized DEIM based HOID

Require: $\mathcal{X} \in \mathbb{R}^{I_1 \times I_2 \times \cdots \times I_d}$, multilinear rank (r_1, r_2, \dots, r_d) and oversampling parameter p .

- 1: **for** $n = 1, 2, \dots, d$ **do**
 - 2: Draw random Gaussian matrix $\Omega \in \mathbb{R}^{(r_n+p) \times I_n}$.
 - 3: Compute $Y = \Omega X_{(n)} \in \mathbb{R}^{(r_n+p) \times \prod_{k \neq n} I_k}$.
 - 4: Compute the SVD of Y^T , $Y^T = ZMK^T$,
 - 5: where $Z \in \mathbb{R}^{\prod_{k \neq n} I_k \times (r_n+p)}$ and $W \in \mathbb{R}^{(r_n+p) \times (r_n+p)}$ are orthonormal, and $\Sigma \in \mathbb{R}^{(r_n+p) \times (r_n+p)}$ is diagonal.
 - 6: Form $Q = Z(:, 1 : r_n)$.
 - 7: Compute $T = X_{(n)}Q$.
 - 8: Compute the SVD of T , $T = V\Sigma U^T$,
 - 9: where $V \in \mathbb{R}^{I_n \times r_n}$ and $U \in \mathbb{R}^{r_n \times r_n}$ are orthonormal, and $\Sigma \in \mathbb{R}^{r_n \times r_n}$ is diagonal.
 - 10: Compute $W_n = QU \in \mathbb{R}^{\prod_{k \neq n} I_k \times r_n}$.
 - 11: **for** $j = 1, 2, \dots, r_n$ **do**
 - 12: $\mathbf{s}(j) = \operatorname{argmax}_{1 \leq i \leq \prod_{k \neq n} I_k} |(W_n(i, j))|$.
 - 13: $W_n(:, j+1) = W_n(:, j+1) - W_n(:, 1:j) \cdot (W_n(\mathbf{s}, 1:j) \backslash W_n(\mathbf{s}, j+1))$.
 - 14: **end for**
 - 15: $C_n = X_n(:, \mathbf{s})$.
 - 16: **end for**
 - 17: Compute the core tensor $\mathcal{G} \in \mathbb{R}^{r_1 \times r_2 \times \cdots \times r_d}$ as $\mathcal{G} = \mathcal{X} \times_1 C_1^\dagger \times_2 C_2^\dagger \cdots \times_d C_d^\dagger$.
 - 18: **return** Tucker decomposition $\hat{\mathcal{X}} = \mathcal{G} \times_1 C_1 \times_2 C_2 \cdots \times_d C_d$.
-

Theorem 4.1. Let $\mathcal{X} \in \mathbb{R}^{I_1 \times I_2 \times \dots \times I_d}$ with $I_n \leq \prod_{k \neq n} I_k$ for $n = 1, 2, \dots, d$, and $\hat{\mathcal{X}}$ be an approximation for \mathcal{X} provided by Algorithm 4. Suppose that p is an oversampling parameter, β and γ are positive numbers such that $\gamma > 1$, and $\phi = \prod_{n=1}^d \chi_n$ with

$$\chi_n = 1 - \frac{1}{\sqrt{2\pi(p+1)}} \left(\frac{e}{(p+1)\beta} \right)^{p+1} - \frac{1}{2(\gamma^2 - 1)\sqrt{\pi I_n \gamma^2}} \left(\frac{2\gamma^2}{e^{\gamma^2 - 1}} \right)^{I_n}.$$

Then

$$\|\mathcal{X} - \hat{\mathcal{X}}\|_F^2 \leq \sum_{n=1}^d \left[I_n \left(\prod_{k \neq n} I_k \right) \left(\frac{r_n \cdot 4^{r_n}}{3} \right) \left(2\sqrt{2(r_n + p)I_n \beta^2 \gamma^2 + 1} + 2\sqrt{2(r_n + p)I_n \beta \gamma} \right)^2 \right] \sigma_{r_n+1}^2$$

holds with probability not less than ϕ , where σ_{r_n+1} is the $(r_n + 1)$ th largest singular value of the mode- n tensor unfolding $X_{(n)}$.

Proof. First, from Lemma 3.1, we have

$$\|\mathcal{X} - \mathcal{G} \times_1 C_1 \times_2 C_2 \cdots \times_d C_d\|_F^2 \leq \sum_{n=1}^d \left(I_n \|(I - C_n C_n^\dagger) X_{(n)}\|_2^2 \right). \quad (4.3)$$

According to Algorithm 4, for $X_{(n)}$, $n = 1, 2, \dots, d$, we have the approximate SVD

$$X_{(n)} = V_n \Sigma W_n^T + E_n,$$

where W_n contains r_n approximated right singular vectors, and the error $\|E_n\|$ satisfies (4.1) with probability not less than (4.2). Suppose that the column indices \mathbf{s} give the full rank matrices $C = X_{(n)} S$ where $S = I(:, \mathbf{s})$, and let $\mathbb{S} = S(W_n^T S)^{-1} W_n^T$ be the interpolatory projectors. Then, using the result in [40, Lemma 4.2], we have

$$\|(I - C C^\dagger) X_{(n)}\| \leq \|X_{(n)}(I - \mathbb{S})\|.$$

Note that $W_n^T W_n = I$. According to [40, Lemma 4.1], we obtain that

$$\|X_{(n)}(I - \mathbb{S})\| \leq \|(W_n^T S)^{-1}\| \|X_{(n)}(I - W_n W_n^T)\|.$$

Then it follows that

$$\begin{aligned} \|(I - C C^\dagger) X_{(n)}\| &\leq \|(W_n^T S)^{-1}\| \|X_{(n)}(I - W_n W_n^T)\| \\ &= \|(W_n^T S)^{-1}\| \|(E_n + V_n \Sigma W_n^T)(I - W_n W_n^T)\| \\ &\leq \|(W_n^T S)^{-1}\| \|E_n(I - W_n W_n^T)\| \leq \|(W_n^T S)^{-1}\| \|E_n\|. \end{aligned}$$

For the DEIM, it is shown in [40, Lemma 4.4] that $\|(W_n^T S)^{-1}\| \leq \sqrt{\frac{r_n \prod_{k \neq n} I_k}{3}} 2^{r_n}$, which implies that

$$\|(I - C C^\dagger) X_{(n)}\| \leq \sqrt{\frac{r_n \prod_{k \neq n} I_k}{3}} 2^{r_n} \left(2\sqrt{2(r_n + p)I_n \beta^2 \gamma^2 + 1} + 2\sqrt{2(r_n + p)I_n \beta \gamma} \right) \sigma_{r_n+1} \quad (4.4)$$

for $n = 1, 2, \dots, d$ with probability not less than

$$\chi_n = 1 - \frac{1}{\sqrt{2\pi(p+1)}} \left(\frac{e}{(p+1)\beta} \right)^{p+1} - \frac{1}{2(\gamma^2 - 1)\sqrt{\pi I_n \gamma^2}} \left(\frac{2\gamma^2}{e^{\gamma^2 - 1}} \right)^{I_n}.$$

Setting $\phi = \prod_{n=1}^d \chi_n$ and inserting relation (4.4) into (4.3), we obtain the the desired error bound. \square

As pointed out in [37], given matrix $X \in \mathbb{R}^{m \times n}$, the relationship between the HOID and the matrix CUR factorization can be established effortlessly by recognizing the subsequent identity:

$$X = CUR + E \iff X = U \times_1 C \times_2 R + E, \quad (4.5)$$

where matrices $C \in \mathbb{R}^{m \times r}$ and $R \in \mathbb{R}^{r \times n}$ are formed by extracting the rows/columns of X . By adopting this specific intersection matrix, the correlation with the core tensor calculation can be derived:

$$U = C^\dagger X R^\dagger \iff U = X \times_1 C^\dagger \times_2 R^\dagger. \quad (4.6)$$

From relations (4.5) and (4.6), it becomes evident that Algorithm 4 can also be applied to produce a matrix CUR decomposition and we summarize the error bound in the following corollary.

Corollary 4.1. *Apply Algorithm 4 to produce the CUR decomposition of $X \in \mathbb{R}^{m \times n}$, $n \geq m$ as in (4.5). Then*

$$\|E\| \leq \left(\sqrt{\frac{mr}{3}} 2^r + \sqrt{\frac{nr}{3}} 2^r \right) \left(2\sqrt{2(r+p)m\beta^2\gamma^2 + 1} + 2\sqrt{2(r+p)m\beta\gamma} \right) \sigma_{r+1}$$

with success probability not less than χ^2 .

4.2 Randomization for L-DEIM based matrix CUR decomposition

We now focus on the integration of random sampling techniques with the L-DEIM algorithm, a combination that can yield good bounds with high probability at a trivial computational cost. To develop a framework for our randomized approaches, firstly, we consider the matrix case and derive a randomized algorithm for the matrix CUR decomposition of the form (1.1).

Suppose the selected indices are stored in the vectors $\mathbf{q}, \mathbf{p} \in \mathbb{N}^r$ so that $C = X(:, \mathbf{q})$ and $R = X(\mathbf{p}, :)$. Our choice for \mathbf{p} and \mathbf{q} is guided by information of the approximate rank- \hat{r} SVD of $X \in \mathbb{R}^{m \times n}$ such that

$$X \approx V \Sigma W^T, \quad (4.7)$$

where matrices W, V contain the leading \hat{r} right and left singular vectors and $\hat{r} \leq r$ is the user-specified parameter contained in the L-DEIM algorithm. Furthermore, we compute decomposition (4.7) by applying the randomized technique, achieving the error (4.1) with probability not less than (4.2). Then we compute

$$U = C^\dagger X R^\dagger, \quad (4.8)$$

yielding a CUR factorization by two steps: first, the columns of X are projected onto the range of C $\text{Ran}(C)$; then the result is projected onto the row space of R . This option minimizes $\|X - CUR\|$ for the given the sampling indices.

Lines 1 to 9 of Algorithm 5 correspond to the construction of rank- \hat{r} truncated SVD of X . Additionally, in line 2, we multiply the matrix X by an $(\hat{r} + p) \times n$ Gaussian matrix Ω to implement truncation, and it would increase to $(r + p) \times n$ if we apply the DEIM, which can be easily observed from line 3 of Algorithm 4. Therefore, by exploiting the L-DEIM technique, the random sampling procedure can be executed very efficiently by achieving a better truncation, which is the primary source of the excellent performance of our approach. Besides, it is worth noting that lines 10 to 19 can be parallelized, as it involves three independent runs of L-DEIM, which operate on the singular vector matrices W and V to select the row indices \mathbf{q} and column indices \mathbf{p} respectively. The following theorem quantifies the error of the rank- r CUR decomposition produced by Algorithm 5.

Algorithm 5 Randomized L-DEIM based CUR decomposition

Require: $X \in \mathbb{R}^{m \times n}$, desired rank r and the specified parameter \hat{r} .

- 1: Draw random Gaussian matrix $\Omega \in \mathbb{R}^{(\hat{r}+p) \times n}$.
 - 2: Compute $Y = \Omega X \in \mathbb{R}^{(\hat{r}+p) \times n}$.
 - 3: Compute the SVD of Y^T , $Y^T = ZMK^T$,
 - 4: where $Z \in \mathbb{R}^{n \times (\hat{r}+p)}$ and $K \in \mathbb{R}^{(\hat{r}+p) \times (\hat{r}+p)}$ are orthonormal, and $M \in \mathbb{R}^{(\hat{r}+p) \times (\hat{r}+p)}$ is diagonal.
 - 5: Form $Q = Z(:, 1 : \hat{r})$.
 - 6: Compute $T = XQ \in \mathbb{R}^{m \times \hat{r}}$.
 - 7: Compute the SVD of T , $T = V\Sigma U^T$,
 - 8: where $V \in \mathbb{R}^{m \times \hat{r}}$ and $U \in \mathbb{R}^{\hat{r} \times \hat{r}}$ are orthonormal, and $\Sigma \in \mathbb{R}^{\hat{r} \times \hat{r}}$ is diagonal.
 - 9: Compute $W = QU \in \mathbb{R}^{n \times \hat{r}}$.
 - 10: **for** $j = 1, 2, \dots, \hat{r}$ **do**
 - 11: $\mathbf{p}(j) = \operatorname{argmax}_{1 \leq i \leq m} |(V(i, j))|$.
 - 12: $V(:, j+1) = V(:, j+1) - V(:, 1:j) \cdot (V(\mathbf{p}, 1:j) \setminus V(\mathbf{p}, j+1))$.
 - 13: **end for**
 - 14: Compute $\ell_i = \|V(i, :)\|$ for $i = 1, 2, \dots, m$.
 - 15: Sort ℓ in non-increasing order.
 - 16: Remove entries in ℓ corresponding to the indices in \mathbf{p} .
 - 17: $\mathbf{p}' = r - \hat{r}$ indices corresponding to $r - \hat{r}$ largest entries of ℓ .
 - 18: $\mathbf{p} = [\mathbf{p}; \mathbf{p}']$.
 - 19: Repeat step 10-18 for W to obtain index set \mathbf{q} .
 - 20: Form $C = X(:, \mathbf{q})$ and $R = X(\mathbf{p}, :)$.
 - 21: Compute $U = C^\dagger X R^\dagger$.
 - 22: **return** CUR decomposition $X \approx CUR$.
-

Theorem 4.2. Let $X \in \mathbb{R}^{m \times n}$ with $n \geq m$. Suppose that p is an oversampling parameter, β and γ are positive numbers such that $\gamma > 1$, and

$$\chi = 1 - \frac{1}{\sqrt{2\pi(p+1)}} \left(\frac{e}{(p+1)\beta} \right)^{p+1} - \frac{1}{2(\gamma^2 - 1)\sqrt{\pi m \gamma^2}} \left(\frac{2\gamma^2}{e^{\gamma^2 - 1}} \right)^m.$$

Then

$$\|X - CUR\| \leq 2^{\hat{r}} \left(\sqrt{\frac{n\hat{r}}{3}} + \sqrt{\frac{m\hat{r}}{3}} \right) \left(2\sqrt{2(\hat{r}+p)m\beta^2\gamma^2 + 1} + 2\sqrt{2(\hat{r}+p)m\beta\gamma} \right) \sigma_{\hat{r}+1}$$

holds with probability not less than χ^2 , where $\sigma_{\hat{r}+1}$ is the $(\hat{r}+1)$ th largest singular value of X .

Proof. This proof is a minor modification of that of [40, Lemma 4.2]. Here we closely follow their proof technique. From the definition of U of (4.8),

$$X - CUR = X - CC^\dagger X R^\dagger R = (I - CC^\dagger)A + CC^\dagger X(I - R^\dagger R).$$

Then we have

$$\begin{aligned} \|X - CUR\| &\leq \|(I - CC^\dagger)X\| + \|CC^\dagger\| \|X(I - R^\dagger R)\| \\ &= \|(I - CC^\dagger)X\| + \|X(I - R^\dagger R)\|, \end{aligned} \tag{4.9}$$

since $\|CC^\dagger\| = 1$. Let $P = I(:, \mathbf{p})$, $Q = I(:, \mathbf{q})$, and $\mathbb{P} = V(P^T V)^\dagger P^T$, $\mathbb{Q} = Q(W^T Q)^\dagger W^T$ be the interpolatory projectors. Using the formula $C = X(:, \mathbf{q}) = XQ$, we have

$$C^\dagger = (C^T C)^{-1} C^T = (Q^T X^T X Q)^{-1} (XQ)^T,$$

and then the orthogonal projection of X onto $\text{Ran}(C)$ is

$$CC^\dagger X = XQQ^\top X^\top XQ^{-1}Q^\top X^\top X.$$

Hence the error in the orthogonal projection of X is

$$(I - CC^\dagger)X = X(I - \Phi), \quad \Phi = Q(Q^\top X^\top XQ)^{-1}Q^\top X^\top X.$$

It is easy to verify that $\Phi Q = Q$. Therefore, we obtain

$$\Phi Q = \Phi Q(W^\top W)^\dagger W^\top = Q(W^\top Q)^\dagger W^\top = Q,$$

which implies that

$$X(I - \Phi) = X(I - \Phi)(I - Q) = (I - CC^\dagger)X(I - Q).$$

Then it follows that

$$\begin{aligned} \|(I - CC^\dagger)X\| &= \|X(I - \Phi)\| \\ &= \|(I - CC^\dagger)X(I - Q)\| \\ &\leq \|I - CC^\dagger\| \|X(I - Q)\| = \|X(I - Q)\|. \end{aligned} \tag{4.10}$$

Analogous manipulation gives

$$\|X(I - R^\dagger R)\| \leq \|(I - \mathbb{P})X\|. \tag{4.11}$$

Note that oblique projectors \mathbb{P} and \mathbb{Q} have the properties $\mathbb{P}V = V$ and $W^\top \mathbb{Q} = W^\top$, so that $(I - \mathbb{P})V = 0$ and $W^\top(I - \mathbb{Q}) = 0$. Therefore,

$$\|X - \mathbb{P}X\| = \|(I - \mathbb{P})X\| = \|(I - \mathbb{P})(I - VV^\top)X\| \leq \|(I - VV^\top)X\| \|(I - \mathbb{P})\|, \tag{4.12}$$

$$\|X - X\mathbb{Q}\| = \|X(I - \mathbb{Q})\| = \|X(I - WW^\top)(I - \mathbb{Q})\| \leq \|X(I - WW^\top)\| \|(I - \mathbb{Q})\|. \tag{4.13}$$

According to the description of the randomized SVD, the error E between matrix $X \in \mathbb{R}^{m \times n}$ and its approximation satisfies the following inequality

$$\|E\| = \|X - XQQ^\top\| \leq \left(2\sqrt{2(\hat{r} + p)m\beta^2\gamma^2 + 1} + 2\sqrt{2(\hat{r} + p)m\beta\gamma}\right) \sigma_{\hat{r}+1}$$

with probability not less than χ as defined in (4.1). Therefore,

$$\begin{aligned} \|(I - VV^\top)X\| &= \|(I - VV^\top)(XQQ^\top + E)\| \\ &\leq \|(I - VV^\top)XQQ^\top + (I - VV^\top)E\| \\ &\leq \|(I - VV^\top)XQQ^\top\| + \|E\| = \|E\|, \end{aligned} \tag{4.14}$$

since $(I - VV^\top)XQQ^\top = (I - VV^\top)V\Sigma W^\top = 0$. A similar treatment shows that

$$\|X(I - WW^\top)\| \leq \|E\| \tag{4.15}$$

with probability not less than χ . Finally, combining the results from [41] and [24] that

$$\|I - \mathbb{P}\| = \|\mathbb{P}\| = \|(P^\top V)^\dagger\| \leq \sqrt{\frac{m\hat{r}}{3}} 2^{\hat{r}}, \quad \|I - \mathbb{Q}\| = \|\mathbb{Q}\| = \|(W^\top Q)^\dagger\| \leq \sqrt{\frac{n\hat{r}}{3}} 2^{\hat{r}},$$

and the relations (4.9)-(4.15), we obtain the desired error bound. \square

4.3 Randomization for L-DEIM based HOID

In this subsection, we design an efficient randomized algorithm for computing a CUR-type factorization for tensors in the Tucker format based on the L-DEIM procedure, which can be viewed as a generalization of Algorithm 5. In this circumstance, each mode of tensor $\mathcal{X} \in \mathbb{R}^{I_1 \times I_2 \times \dots \times I_d}$ is processed separately. Specifically, the factor matrices $C_n = X_{(n)}(:, \mathbf{s})$ are constructed by extracting r_n columns from the n -mode unfolding $X_{(n)}$, where \mathbf{s} represents the index sets of the selected columns. The selection of \mathbf{s} is achieved by applying the L-DEIM algorithm to the approximate right singular matrices W_n , computed by employing the random sampling method as described in Section 4.1. Once all factor matrices $\{C_n\}_{n=1}^d$ are obtained, the core tensor is formed as

$$\mathcal{G} = \mathcal{X} \times_1 C_1^\dagger \times_2 C_2^\dagger \cdots \times_d C_d^\dagger.$$

Algorithm 6 is a summary of this procedure and it has several advantages: (1) it returns a HOID factorization that is known to be more interpretable than the HOSVD as it corresponds to representing data via other actual data points; (2) it has a computational advantage: the main cost of the random truncation process presented in lines 2 to 10 of Algorithm 4 comes from the SVD computation and it needs $\mathcal{O}\left((r_i + p)^2 \prod_{k \neq i} I_k + I_i r_i^2\right)$. Since it requires fewer singular vectors in Algorithm 6, it reduces to $\mathcal{O}\left((\hat{r}_i + p)^2 \prod_{k \neq i} I_k + I_i \hat{r}_i^2\right)$. (3) there is a good theoretical guarantee for its performance, and we establish it in the following theorem.

Algorithm 6 Randomized L-DEIM based HOID

Require: $\mathcal{X} \in \mathbb{R}^{I_1 \times I_2 \times \dots \times I_d}$, multilinear rank (r_1, r_2, \dots, r_d) and parameters $(\hat{r}_1, \hat{r}_2, \dots, \hat{r}_d)$.

- 1: **for** $n = 1, 2, \dots, d$ **do**
 - 2: Draw random Gaussian matrix $\Omega \in \mathbb{R}^{(\hat{r}_n + p) \times I_n}$.
 - 3: Compute $Y = \Omega X_{(n)} \in \mathbb{R}^{(\hat{r}_n + p) \times \prod_{k \neq n} I_k}$.
 - 4: Compute the SVD of Y^T , $Y^T = ZMK^T$,
 - 5: where $Z \in \mathbb{R}^{\prod_{k \neq n} I_k \times (\hat{r}_n + p)}$ and $W \in \mathbb{R}^{(\hat{r}_n + p) \times (\hat{r}_n + p)}$ are orthonormal, and $\Sigma \in \mathbb{R}^{(\hat{r}_n + p) \times (\hat{r}_n + p)}$ is diagonal.
 - 6: Form $Q = Z(:, 1 : \hat{r}_n)$.
 - 7: Compute $T = X_{(n)} Q$.
 - 8: Compute the SVD of T , $T = V \Sigma U^T$,
 - 9: where $V \in \mathbb{R}^{I_n \times \hat{r}_n}$ and $U \in \mathbb{R}^{\hat{r}_n \times \hat{r}_n}$ are orthonormal, and $\Sigma \in \mathbb{R}^{\hat{r}_n \times \hat{r}_n}$ is diagonal.
 - 10: Compute $W_n = Q U \in \mathbb{R}^{\prod_{k \neq n} I_k \times \hat{r}_n}$
 - 11: **for** $j = 1, 2, \dots, \hat{r}_n$ **do**
 - 12: $\mathbf{s}(j) = \arg\max_{1 \leq i \leq \prod_{k \neq n} I_k} |(W_n(i, j))|$.
 - 13: $W_n(:, j+1) = W_n(:, j+1) - W_n(:, 1:j) \cdot (W_n(\mathbf{s}, 1:j) \setminus W_n(\mathbf{s}, j+1))$.
 - 14: **end for**
 - 15: Compute $\ell_i = \|W_n(i, :)\|$ for $i = 1, 2, \dots, I_n$.
 - 16: Sort ℓ in non-increasing order.
 - 17: Remove entries in ℓ corresponding to the indices in \mathbf{s} .
 - 18: $\mathbf{s}' = r_n - \hat{r}_n$ indices corresponding to $r_n - \hat{r}_n$ largest entries of ℓ .
 - 19: $\mathbf{s} = [\mathbf{s}; \mathbf{s}']$.
 - 20: Form $C_n = X_{(n)}(:, \mathbf{s})$.
 - 21: **end for**
 - 22: Compute core tensor $\mathcal{G} \in \mathbb{R}^{r_1 \times \dots \times r_d}$ as $\mathcal{G} = \mathcal{X} \times_1 C_1^\dagger \times_2 C_2^\dagger \cdots \times_d C_d^\dagger$.
 - 23: **return** Tucker decomposition $\mathcal{X} \approx \mathcal{G} \times_1 C_1 \times_2 C_2 \cdots \times_d C_d$.
-

Theorem 4.3. Let $\mathcal{X} \in \mathbb{R}^{I_1 \times I_2 \times \dots \times I_d}$ with $I_n \leq \prod_{k \neq n} I_k$ for $n = 1, 2, \dots, d$. Suppose that p is an

oversampling parameter, β and γ are positive numbers such that $\gamma > 1$, and $\phi = \prod_{n=1}^d \chi_n$ with

$$\chi_n = 1 - \frac{1}{\sqrt{2\pi(p+1)}} \left(\frac{e}{(p+1)\beta} \right)^{p+1} - \frac{1}{2(\gamma^2-1)\sqrt{\pi I_n \gamma^2}} \left(\frac{2\gamma^2}{e^{\gamma^2-1}} \right)^{I_n}.$$

Then Algorithm 6 provides a multilinear rank (r_1, r_2, \dots, r_d) approximation for tensor \mathcal{X} with the following error bound which holds with probability not less than ϕ

$$\begin{aligned} \|\mathcal{X} - \mathcal{G} \times_1 C_1 \times_2 C_2 \cdots \times_d C_d\|_F^2 &\leq \sum_{n=1}^d \left[I_n \left(\prod_{k \neq n} I_k \right) \left(\frac{\hat{r}_n \cdot 4^{\hat{r}_n}}{3} \right) \left(2\sqrt{2(\hat{r}_n + p) I_n \beta^2 \gamma^2 + 1} \right. \right. \\ &\quad \left. \left. + 2\sqrt{2(\hat{r}_n + p) I_n \beta \gamma} \right)^2 \right] \sigma_{\hat{r}_n+1}^2. \end{aligned}$$

Proof. By Lemma 3.1, the error in \mathcal{X} is bounded by the sum of the error in each mode, i.e.,

$$\|\mathcal{X} - \mathcal{G} \times_1 C_1 \times_2 C_2 \cdots \times_d C_d\|_F^2 \leq \sum_{n=1}^d \left(I_n \|(I - C_n C_n^\dagger) X_{(n)}\|_2^2 \right). \quad (4.16)$$

Applying the results of Theorem 4.2, we have

$$\begin{aligned} \|(I - C_n C_n^\dagger) X_{(n)}\|^2 &\leq \left(\prod_{k \neq n} I_k \right) \left(\frac{\hat{r}_n 4^{\hat{r}_n}}{3} \right) \left(2\sqrt{2(\hat{r}_n + p) I_n \beta^2 \gamma^2 + 1} \right. \\ &\quad \left. + 2\sqrt{2(\hat{r}_n + p) I_n \beta \gamma} \right)^2 \sigma_{\hat{r}_n+1}^2, \end{aligned} \quad (4.17)$$

with probability not less than $\chi_n = 1 - \frac{1}{\sqrt{2\pi(p+1)}} \left(\frac{e}{(p+1)\beta} \right)^{p+1} - \frac{1}{2(\gamma^2-1)\sqrt{\pi I_n \gamma^2}} \left(\frac{2\gamma^2}{e^{\gamma^2-1}} \right)^{I_n}$. Setting $\phi = \prod_{n=1}^d \chi_n$ and plugging inequality (4.17) into (4.16), we obtain the desired result. \square

5 Randomization for hybrid decomposition

This subsection develops the randomized algorithms for computing the hybrid CUR-type decomposition of the form (2.3).

The essence of the hybrid decomposition is that we retain the fibers of the original tensor in only one mode, or in more, but not all modes. Specifically, as in (2.3), the fibers from the first t modes are preserved in matrices $\{C_i\}_{i=1}^t$, which are the representative of the mode- i unfolding matrices $X_{(i)}$, and matrices $\{U_j\}_{j=t+1}^d$ which contain first r_j left singular vectors of $X_{(j)}$ are chosen to minimize the approximation error. We summarize the hybrid approach in Algorithm 7 for the case that only the first mode of the original fibers is preserved. Alternatively, we may opt to extract fibers from multiple modes, while noting that the reduction in the number of preserved original fibers correlates with an increase in the resulting error.

In Algorithm 7, the factor matrix C is derived by performing PQR to the mode-1 unfolding, while other sampling techniques, such as the RRQR, DEIM and L-DEIM can also be employed. Nevertheless, the precise computation of the PQR or the singular matrices of $X_{(n)}$ can be excessively costly, thereby posing a challenge for large-scale applications. Here we adopt random sampling techniques to tackle this difficulty. Given matrix $X \in \mathbb{R}^{m \times n}$ with $n \geq m$, the randomized algorithm in [34] yields an approximate interpolatory decomposition with the error bound

$$\|CU - X\|_2 \leq (\sqrt{2lm\beta^2\gamma^2 + 1}(\sqrt{4k(n-k) + 1} + 1) + \beta\gamma\sqrt{2lm}\sqrt{4k(n-k) + 1})\sigma_{k+1}, \quad (5.1)$$

Algorithm 7 Hybrid algorithm [6]

Require: $\mathcal{X} \in \mathbb{R}^{I_1 \times I_2 \times \dots \times I_d}$ and desired multilinear rank (r_1, r_2, \dots, r_d) .

- 1: **for** $i = 2, 3, \dots, d$ **do**
- 2: Compute matrix U_i containing the leading r_i left singular vectors of $X_{(i)}$.
- 3: **end for**
- 4: Perform the PQR decomposition $X_{(1)}P = QR$.
- 5: Compute factor matrix $C = X_{(1)}P(:, 1 : r_1) \in \mathbb{R}^{n_1 \times r_1}$.
- 6: Compute core tensor $\mathcal{G} \in \mathbb{R}^{r_1 \times \dots \times r_d}$ as

$$\mathcal{G} = \mathcal{X} \times_1 C^\dagger \times_2 U_2^T \dots \times_d U_d^T.$$

- 7: **return** tensor hybrid decomposition $\mathcal{X} \approx \mathcal{G} \times_1 C \times_2 U_2 \dots \times_d U_d$
-

with probability not less than χ , where χ , β and γ are defined as in (4.1) and (4.2). Computational complexity analysis and numerical examples illustrate this method can accelerate the approximation of matrices significantly. We present our approach in Algorithm 8, where we exploit the randomization techniques to accelerate the process of the SVD and the interpolatory decomposition to each mode unfolding, providing an approximation $\hat{\mathcal{X}}$ in a hybrid CUR-type Tucker format for a given tensor \mathcal{X} such that

$$\hat{\mathcal{X}} = \mathcal{G} \times_1 C_1 \dots \times_t C_t \times_{t+1} U_{t+1} \dots \times_d U_d.$$

The following theorem quantifies the error of the approximate hybrid CUR-type Tucker decomposition produced by Algorithm 8.

Algorithm 8 Randomized hybrid algorithm based the PQR

Require: $\mathcal{X} \in \mathbb{R}^{I_1 \times I_2 \times \dots \times I_d}$, multilinear rank (r_1, r_2, \dots, r_d) and oversampling parameter p .

- 1: **for** $i = 1, 2, \dots, t$ **do**
 - 2: Draw random Gaussian matrix $\Omega \in \mathbb{R}^{(r_i+p) \times I_i}$.
 - 3: Compute $Y = \Omega X_{(i)}$.
 - 4: Apply the pivoted Gram-Schmidt process to the columns of Y , $YP = QR$, where $P \in \mathbb{R}^{(\prod_{k \neq i} n_k) \times (\prod_{k \neq i} n_k)}$, P is a permutation matrix, $Q \in \mathbb{R}^{(r_i+p) \times r_i}$ is orthonormal, and $R \in \mathbb{R}^{r_i \times \prod_{k \neq i} I_k}$ is upper triangular.
 - 5: Form $C_i = X_{(i)}P(:, 1 : r_i)$.
 - 6: **end for**
 - 7: **for** $j = t+1, t+2, \dots, d$ **do**
 - 8: Draw random Gaussian matrix $\Omega \in \mathbb{R}^{(r_j+p) \times I_j}$.
 - 9: Compute $M = \Omega X_{(j)}$.
 - 10: Compute the SVD of M , $M = Z\Sigma V^T$, where $Z \in \mathbb{R}^{\prod_{k \neq j} I_k \times (r_j+p)}$ and $V \in \mathbb{R}^{(r_j+p) \times (r_j+p)}$ are orthonormal, and $\Sigma \in \mathbb{R}^{(r_j+p) \times (r_j+p)}$ is diagonal.
 - 11: Form $Q = Z(:, 1 : r_j)$.
 - 12: Compute $T = X_{(j)}Q$.
 - 13: Compute matrix U_j containing r_j left singular vectors of $X_{(j)}$.
 - 14: **end for**
 - 15: Compute the core tensor $\mathcal{G} \in \mathbb{R}^{r_1 \times r_2 \times \dots \times r_d}$ as $\mathcal{G} = \mathcal{X} \times_1 C_1^\dagger \dots \times_t C_t^\dagger \times_{t+1} U_{t+1}^T \dots \times_d U_d^T$.
-

Theorem 5.1. Let $\mathcal{X} \in \mathbb{R}^{I_1 \times I_2 \times \dots \times I_d}$ with $I_n \leq \prod_{k \neq n} I_k$ for $1 \leq n \leq d$. Suppose that p is an oversampling parameter, β and γ are positive numbers such that $\gamma > 1$, and

$$\chi_n = 1 - \frac{1}{\sqrt{2\pi(p+1)}} \left(\frac{e}{(p+1)\beta} \right)^{p+1} - \frac{1}{2(\gamma^2-1)\sqrt{\pi I_n \gamma^2}} \left(\frac{2\gamma^2}{e\gamma^2-1} \right)^{I_n}. \quad (5.2)$$

Then Algorithm 8 produces a hybrid decomposition with the following error bound,

$$\begin{aligned} \|\mathcal{X} - \hat{\mathcal{X}}\|_F^2 &\leq \sum_{i=1}^t I_i \left[\sqrt{2(r_i + p)I_i\beta^2\gamma^2 + 1} \left(\sqrt{4r_i(\prod_{k \neq i} I_k - r_i) + 1} + 1 \right) \right. \\ &\quad \left. + \beta\gamma\sqrt{2(r_i + p)I_i} \sqrt{4r_i(\prod_{k \neq i} I_k - r_i) + 1} \right]^2 \sigma_{r_i+1}^2 \\ &\quad + \sum_{j=t+1}^d I_j \left(2\sqrt{2(r_j + p)I_j\beta^2\gamma^2 + 1} + 2\sqrt{2(r_j + p)I_j}\beta\gamma \right)^2 \sigma_{r_j+1}^2 \end{aligned} \quad (5.3)$$

with probability not less than $\phi = \prod_{n=1}^d \chi_n$, where σ_{r_i+1} is the $(r_i + 1)$ th largest singular value of $X_{(i)}$.

Proof. Using the property of the mode- n product, we have

$$\|\mathcal{X} - \hat{\mathcal{X}}\|_F^2 = \|\mathcal{X} - \mathcal{X} \times_1 (C_1 C_1^\dagger) \times_2 \cdots \times_t (C_t C_t^\dagger) \times_{t+1} (U_{t+1} U_{t+1}^\top) \times \cdots \times_d (U_d U_d^\top)\|_F^2.$$

Notice that $C_i C_i^\dagger$ and $U_j U_j^\top$ are orthogonal projections. Recalling the result in [40, Lemma 2.1], for orthogonal projections $\{\Pi_i\}_{i=1}^n$, we have

$$\|\mathcal{X} - \mathcal{X} \times_1 \Pi_1 \times_2 \Pi_2 \cdots \times_d \Pi_d\|_F^2 \leq \sum_{i=1}^d \|\mathcal{X} - \mathcal{X} \times_i \Pi_i\|_F^2,$$

then it follows that

$$\begin{aligned} \|\mathcal{X} - \hat{\mathcal{X}}\|_F^2 &\leq \sum_{i=1}^t \|\mathcal{X} - \mathcal{X} \times_i (C_i C_i^\dagger)\|_F^2 + \sum_{j=t+1}^d \|\mathcal{X} - \mathcal{X} \times_j (U_j U_j^\top)\|_F^2 \\ &= \sum_{i=1}^t \|(I - C_i C_i^\dagger)X_{(i)}\|_F^2 + \sum_{j=t+1}^d \|(I - U_j U_j^\top)X_{(j)}\|_F^2. \end{aligned} \quad (5.4)$$

As described in Algorithm 8, matrices $X_{(i)}, 1 \leq i \leq t$ and $X_{(j)}, t+1 \leq j \leq d$ own the interpolatory factorization $X_{(i)} = C_i B_i + E_i$ and the SVD such that $X_{(j)} = U_j \Sigma_j V_j^\top + H_j$. Therefore,

$$\begin{aligned} \|(I - C_i C_i^\dagger)X_{(i)}\|_F^2 &= \|(I - C_i C_i^\dagger)(C_i B_i + E_i)\|_F^2 = \|(I - C_i C_i^\dagger)E_i\|_F^2 \leq I_i \|E_i\|_2^2, \\ \|(I - U_j U_j^\top)X_{(j)}\|_F^2 &= \|(I - U_j U_j^\top)(U_j \Sigma_j V_j^\top + H_j)\|_F^2 = \|(I - U_j U_j^\top)H_j\|_F^2 \leq I_j \|H_j\|_2^2. \end{aligned}$$

Plugging these two inequalities into (5.4), and using the results in (5.1) and (4.1), we obtain the desired result. \square

Here we also apply the L-DEIM approach for designing a new randomized algorithm to compute the hybrid decomposition. Once again, the randomized SVD algorithm is utilized to speed up the calculations. This method is presented in Algorithm 9. Notice that in Algorithm 9, if we set the parameters $\hat{r}_i = r_i$, for $i = 1, \dots, t$, then this method degenerates to the DEIM induced HOID algorithm. We derive the upper bound for the expected error in the following theorem.

Theorem 5.2. *Let $\hat{\mathcal{X}}$ be an approximation of $\mathcal{X} \in \mathbb{R}^{I_1 \times I_2 \times \cdots \times I_d}$ computed by Algorithm 9. Then the approximation error \mathcal{E} satisfies*

$$\begin{aligned} \|\mathcal{E}\|_F^2 &\leq \sum_{j=t+1}^d I_j \left(2\sqrt{2(r_j + p)I_j\beta^2\gamma^2 + 1} + 2\sqrt{2(r_j + p)I_j}\beta\gamma \right)^2 \sigma_{r_j+1}^2 \\ &\quad + \sum_{i=1}^t I_i \left(\prod_{k \neq i} I_k \right) \left(\frac{\hat{r}_i \cdot 4\hat{r}_i}{3} \right) \left(2\sqrt{2(\hat{r}_i + p)I_i\beta^2\gamma^2 + 1} + 2\sqrt{2(\hat{r}_i + p)I_i}\beta\gamma \right)^2 \sigma_{\hat{r}_i+1}^2, \end{aligned} \quad (5.5)$$

with probability not less than $\phi = \prod_{n=1}^d \chi_n$.

Proof. Firstly, using analogous operation in the proof of Theorem 5.1 yields the following inequality:

$$\|\mathcal{X} - \hat{\mathcal{X}}\|_F^2 \leq \sum_{i=1}^t \|(I - C_i C_i^\dagger) X_{(i)}\|_F^2 + \sum_{j=t+1}^d \|(I - U_j U_j^T) X_{(j)}\|_F^2, \quad (5.6)$$

and it still holds that

$$\|(I - U_j U_j^T) X_{(j)}\|_F^2 \leq I_j \left(2\sqrt{2(r_j + p)I_j \beta^2 \gamma^2 + 1} + 2\sqrt{2(r_j + p)I_j \beta \gamma} \right)^2 \sigma_{r_j+1}^2 \quad (5.7)$$

with probability not less than χ_j .

Secondly, we note that the factor matrices C_i are computed using the same method as in Algorithm 8, which generates the error satisfying that

$$\begin{aligned} \|(I - C_i C_i^\dagger) X_{(i)}\|_F^2 &\leq I_i \left(\prod_{k \neq i} I_k \right) \left(\frac{\hat{r}_i 4^{\hat{r}_i}}{3} \right) \left(2\sqrt{2(\hat{r}_i + p)I_i \beta^2 \gamma^2 + 1} \right. \\ &\quad \left. + 2\sqrt{2(\hat{r}_i + p)I_i \beta \gamma} \right)^2 \sigma_{\hat{r}_i+1}^2, \end{aligned} \quad (5.8)$$

with probability not less than χ_i . Substituting (5.7) and (5.8) into the right-hand side of (5.6), the desired error bound follows. \square

We now comment on the practical aspects of the algorithms. One can observe that the randomized hybrid algorithms described above can be split naturally into two computational steps. The first step is to construct matrices C_i for the first t modes, where the arithmetic cost comprises the cost of sampling and the cost of computing the SVD or PQR and the latter is actually the most time-consuming operation. The computational complexity of computing SVD in lines 4 and 7 of Algorithm 9 is $\mathcal{O}\left(\prod_{i=1}^t \left[(\hat{r}_i + p)^2 \prod_{k \neq i} I_k + I_i \hat{r}_i^2\right]\right)$, which is much lower to the cost of computing the QR corresponding to line 4 of Algorithm 8. This computational advantage is mainly attributed to the superiority of the L-DEIM procedure, which is crucial, especially for the situation with a large t . In the second step of Algorithms 8, and 9, we exploit the random sampling techniques to obtain U_j , containing r_j right singular vectors which cost $\mathcal{O}\left(\prod_{j=t+1}^d \left[(r_j + p)I_j \prod_{k \neq j} I_k + (r_j + p)^2 \prod_{k \neq j} I_k + I_j r_j^2 + I_j r_j \prod_{k \neq j} I_k\right]\right)$. Numerical experiments in the next section will show that the two algorithms lead to dramatic accelerations in practice, and have the accuracy comparable with the deterministic algorithm.

Algorithm 9 Randomized hybrid algorithm based the L-DEIM

Require: $\mathcal{X} \in \mathbb{R}^{I_1 \times I_2 \times \dots \times I_d}$, multilinear rank (r_1, r_2, \dots, r_d) , parameters $(\hat{r}_1, \dots, \hat{r}_t)$ and oversampling parameter p .

```
1: for  $i = 1, 2, \dots, t$  do
2:   Draw random Gaussian matrix  $\Omega \in \mathbb{R}^{(\hat{r}_i+p) \times I_i}$ .
3:   Compute  $Y = \Omega X_{(i)}$ .
4:   Compute the SVD of  $Y^T$ ,  $Y^T = ZMK^T$ , where  $Z \in \mathbb{R}^{\prod_{k \neq i} I_k \times (\hat{r}_i+p)}$  and  $K \in \mathbb{R}^{(\hat{r}_i+p) \times (\hat{r}_i+p)}$ 
   are orthonormal, and  $M$  is diagonal.
5:   Form  $Q = Z(:, 1 : \hat{r}_i)$ .
6:   Compute  $T = X_{(i)}Q$ .
7:   Compute the the SVD of  $T$ ,  $T = V\Sigma G^T$ , where  $V \in \mathbb{R}^{\prod_{k \neq i} I_k \times (\hat{r}_i+p)}$  and  $G \in \mathbb{R}^{(\hat{r}_i+p) \times (\hat{r}_i+p)}$  are
   orthonormal, and  $\Sigma$  is diagonal.
8:   Compute  $W_i = QG$ .
9:   for  $l = 1, 2, \dots, \hat{r}_i$  do
10:     $\mathbf{s}(l) = \operatorname{argmax}_{1 \leq u \leq \prod_{k \neq i} I_k} |(W_i(u, l))|$ .
11:     $W_i(:, l+1) = W_i(:, l+1) - W_i(:, 1 : l) \cdot (W_i(\mathbf{s}, 1 : l) \setminus W_i(\mathbf{s}, l+1))$ .
12:   end for
13:   Compute  $\ell_u = \|W_u(i, :)\|$  for  $u = 1, 2, \dots, \prod_{k \neq i} I_k$ .
14:   Sort  $\ell$  in non-increasing order.
15:   Remove entries in  $\ell$  corresponding to the indices in  $\mathbf{s}$ .
16:    $\mathbf{s}' = r_i - \hat{r}_i$  indices corresponding to  $r_i - \hat{r}_i$  largest entries of  $\ell$ .
17:    $\mathbf{s} = [\mathbf{s}; \mathbf{s}']$ .
18:    $C_i = X_{(i)}(:, \mathbf{s})$ 
19: end for
20: for  $j = t+1, t+2, \dots, d$  do
21:   Perform line 2-7 to compute matrix  $U_j$  containing  $r_j$  left singular vectors of  $X_{(j)}$ .
22: end for
23: Compute the core tensor  $\mathcal{G} \in \mathbb{R}^{r_1 \times r_2 \times \dots \times r_d}$  as  $\mathcal{G} = \mathcal{X} \times_1 C_1^\dagger \dots \times_t C_t^\dagger \times_{t+1} U_{t+1}^T \dots \times_d U_d^T$ .
```

6 Numerical examples

In this section, we check the accuracy and the computational cost of the proposed algorithms on various synthetic and real-world data sets. All computations are carried out in MATLAB R2020a on a computer with an AMD Ryzen 5 processor and 16 GB RAM. The tensor package in MATLAB, namely Tensor Toolbox [4] is used. For the sake of clarity and consistency, we introduce the following acronyms to facilitate comparisons between different algorithms. The algorithms under consideration operate on the input tensors to produce a Tucker approximation with a multilinear rank (r_1, r_2, \dots, r_d) :

1. HOID— implements the HOID algorithm with column subset selection implemented using either the DEIM algorithm (Algorithm 1) labeled “HOID-DEIM”, or the L-DEIM algorithm (Algorithm 2) labeled “HOID-LDEI” as summarized in Algorithm 3.

2. R-HOID — applies the randomized HOID algorithm with column subset selection implemented using either the DEIM algorithm (Algorithm 1) labeled “R-HOID-DEIM”, summarized in Algorithm 4, or the L-DEIM algorithm (Algorithm 2) labeled “R-HOID-LDEIM” as summarized in Algorithm 6.

3. Hybrid — implements Algorithm 7 to produce the hybrid decomposition.

4. R-Hybrid — implements the randomized hybrid algorithm based on the PQR (Algorithm 8) labeled “R-hybrid-PQR”, and the randomized algorithm based on the DEIM algorithm labeled “R-

hybrid-DEIM”, and the L-DEIM algorithm labeled “R-hybrid-LDEIM” (Algorithm 9) to produce the hybrid decomposition.

Example 6.1 We evaluate the efficacy of the proposed algorithms on the function related tensor below from [6]

$$\mathcal{X}(i_1, i_2, \dots, i_d) = \frac{1}{i_1 + 2 \cdot i_2 + \dots + d \cdot i_d}, \quad 1 \leq i_j \leq I_j \text{ for } j = 1, 2, \dots, d.$$

As described in [6], the utilization of the aforementioned tensor yields an advantage in that the singular values of every mode unfolding of the tensor \mathcal{X} exhibit a rapid decay. This characteristic indicates that tensor \mathcal{X} is highly amenable to the randomized algorithms proposed in this paper. The HOID and Hybrid methods are relevant here because the entries of this tensor are non-negative and we would like to preserve this structure in the column matrices $\{C_i\}$.

We conduct two sets of experiments on tensor \mathcal{X} . Our first experiment compares the accuracy of the HOID algorithms with their randomized counterparts R-HOID. Our inputs consisted of tensor \mathcal{X} with $d = 3$ and $I_j = 100$ for $j = 1, 2, \dots, d$. For each algorithm, we use the target multirank (r, r, r) , where r varies from 1 to 10, and the parameter \hat{r}_n contained in the L-DEIM procedure is $r - 1$ for $r \geq 2$. The same oversampling parameter $p = 5$ is used in every mode. The left section of Figure 1 illustrates the relative error of all four algorithms, demonstrating that their approximation errors are remarkably similar. Notably, the randomized algorithms exhibit impressive accuracy as well. In the subsequent experiment, we compared the accuracy of the Hybrid and R-Hybrid algorithms using a set of inputs with $I_j = 50$ for $j = 1, 2, \dots, d$, and the results are depicted in the right section of Figure 1. Once again, we observed that all four algorithms performed similarly, and the error computed by the R-Hybrid-LDEIM algorithm was only marginally higher than that of the other algorithms.

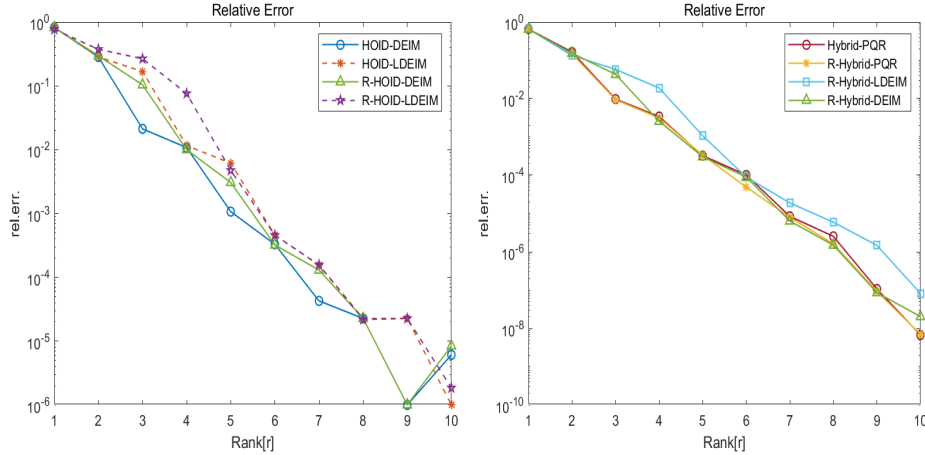


Figure 1: Relative error in the computation of a rank- (r, r, r) approximation to the tensor \mathcal{X} with $d = 3$ and oversampling parameter $p = 5$. Left: computed by the HOID and R-HOID methods with $I_j = 100$ for $j = 1, 2, \dots, d$. Right: computed by the Hybrid and R-Hybrid methods with $I_j = 50$ for $j = 1, 2, \dots, d$.

Our analysis reveals that the randomized variations of our proposed algorithms exhibit significantly lower computational costs in comparison to their deterministic counterparts. To illustrate this, we conducted experiments on tensor \mathcal{X} , gradually increasing the size of each dimension N and the target rank r , and record the CPU time in seconds (denoted as CPU) and the approximation quality (measured by the relative error, Err) of the HOID, R-HOID, Hybrid, and R-Hybrid algorithms. Our investigation begin by comparing the accuracy and CPU time of the HOID algorithms against their randomized equivalents, R-HOID, while holding the oversampling parameter at a fixed value of $p = 5$ for the inputs. According to the conclusions summarized in [23], the L-DEIM procedure may

be comparable to the original DEIM method when the target rank r is at most twice the available \hat{r} singular vectors. Therefore, here we set the parameter $\hat{r}_n, n = 1, 2, \dots, d$ contained in the L-DEIM to be $\hat{r}_n = r_n/2$. We record the results in Table 1. It is clear from the running time that the algorithms R-HOID-DEIM and R-HOID-LDEIM have a huge advantage in computing speed over the non-random HOID method. We also observe that the L-DEIM induced algorithms HOID-LDEIM and R-HOID-LDEIM beat the HOID-DEIM and R-HOID-DEIM algorithms both in terms of accuracy and computational cost.

Then we perform the same set of experiments to show the advantage of the R-Hybrid over the Hybrid method, and we display the relative errors and CPU in Table 2. Table 2 illustrates that the randomized algorithms lead to a dramatic speed-up over the classical nonrandom algorithms, while the R-Hybrid-LDEIM algorithm achieves the smallest running time among the four sets of experiments. We can also see that the approximation errors of all the four algorithms are very close.

Table 1: Comparison of the deterministic algorithms (HOID-DEIM and HOID-LDEIM) and the randomized algorithms (R-HOID-DEIM and R-HOID-LDEIM) in the CPU and relative error as the dimension N and the target rank r increase.

(N, r)		(200, 30)	(300, 30)	(400, 40)	(500, 50)	(600, 40)
HOID-DEIM	Err	1.5436e-04	7.7292e-05	9.5476e-05	5.9806e-05	6.7395e-05
	CPU	11.018	29.077	89.509	189.01	234.53
HOID-LDEIM	Err	9.8135e-07	1.8748e-08	3.1492e-05	1.8460e-05	1.5446e-05
	CPU	4.5589	13.168	37.091	83.891	105.76
R-HOID-DEIM	Err	2.7009e-05	1.2524e-05	2.7430e-05	9.2903e-05	5.0762e-05
	CPU	0.69462	1.7397	4.9565	10.936	12.769
R-HOID-LDEIM	Err	1.2343e-06	6.0400e-08	5.2151e-06	3.6238e-05	3.4919e-05
	CPU	0.39307	1.1647	2.6360	5.8115	7.2012

Table 2: Comparison of the Hybrid and the randomized algorithms (R-Hybrid-PQR, R-Hybrid-DEIM and R-Hybrid-LDEIM) in the CPU and relative error as the dimension N and the target rank r increase.

(N, r)		(100, 20)	(125, 30)	(150, 50)	(200, 30)
Hybrid	Err	2.9535e-07	1.9356e-15	1.7241e-15	2.1394e-15
	CPU	42.122	135.16.3914	69.017	200.31
R-Hybrid-PQR	Err	2.6169e-07	1.5708e-07	1.7312e-15	1.7677e-15
	CPU	0.071084	0.17292	0.97392	0.54113
R-Hybrid-DEIM	Err	1.9946e-07	1.9049e-07	1.8864e-15	2.0811e-15
	CPU	0.077165	0.19325	0.77934	0.60290
R-Hybrid-LDEIM	Err	2.1411e-07	1.6487e-07	1.9008e-15	1.5999e-15
	CPU	0.067160	0.15138	0.72396	0.46221

Example 6.2 Now we check the accuracy and the computational cost of our algorithms on real-world tensors. Our first test problem comes from the classification of handwritten digits images. This problem, popularized by Savas and Eldén in [38], involves assigning a label from 0-9 to a new image representing a handwritten digit. Here we adopt the classification strategy in [37] which relies on the HOID representation and consists of two main steps: a compression phase and a classification phase. In the compression phase, various approaches are applied to a training image dataset arranged as a tensor to compute a low multirank decomposition, while the second step is a classification phase. Our focus in this study is on the first step of efficiently decomposing a tensor formed using images from the MNIST and USPS databases [3]. These databases contain 60,000 images with 28×28 pixels and

1,100 images with 16×16 pixels, both in 8-bit grayscale. The images are unequally distributed over ten classes, but to ensure equal representation across all digits in MNIST, we restrict the number of images in each class to 5,421. Consequently, we organize the images from MNIST and USPS into tensors of size $784 \times 5421 \times 10$ and $256 \times 110 \times 10$, respectively. Here, the first dimension represents the pixels, the second dimension represents the images, and the third dimension represents the digits.

Specifically, we fix the target multirank (r_1, r_2, r_3) to be $(62, 142, 10)$ for the MINST, $(50, 100, 10)$ for the USPS, the oversampling parameter $p = 5$ and the parameter \hat{r}_n contained in the L-DEIM as $r_n/2$ for $n = 1, 2, 3$. For the Hybrid methods, the original fibers only in the first mode are preserved. We report the running time and the relative error of the HOID, Hybrid algorithms and its randomized algorithms in Tables 3 and 4. We observe that the classical algorithm runs almost three times as long as the L-DEIM induced randomized algorithms (R-HOID-LDEIM and R-Hybrid-LDEIM), which also give comparable relative errors. It indicates that using the random sampling techniques and L-DEIM method leads to a dramatic speed-up over classical techniques.

Table 3: Relative error and running time of both HOID and the randomized algorithms R-HOID on the tensors generated from the USPS and MINST database. We set the target multirank (r_1, r_2, r_3) to be $(62, 142, 10)$ for MINST and $(50, 100, 10)$ for the USPS, while the parameter \hat{r}_n contained in the L-DEIM is $r_n/2$ for $n = 1, 2, 3$ and an oversampling parameter of $p = 5$ as inputs.

Method		HOID-DEIM	HOID-LDEIM	R-HOID-DEIM	R-HOID-LDEIM
USPS	Err	0.53785	0.63637	0.56825	0.65947
	CPU	4.3392	2.0040	0.63923	0.34326
MINST	Err	0.54002	0.68095	0.56040	0.70049
	CPU	64.103	32.175	8.8650	4.9925

Table 4: Relative error and running time of both Hybrid, R-Hybrid-PQR, R-Hybrid-DEIM and R-Hybrid-LDEIM on the tensors generated from the USPS and MINST database. The parameters and target multirank are the same as in Table 3 and the original fibers only in the first mode are preserved.

Method		Hybrid	R-hybrid-PQR	R-hybrid-DEIM	R-hybrid-LDEIM
USPS	Err	0.47248	0.52994	0.52791	0.54056
	CPU	1.9945	0.42849	0.49049	0.39817
MINST	Err	0.48134	0.52807	0.51707	0.53724
	CPU	127.55	5.9234	6.5194	5.6317

Example 6.3 We conducted our final test using a formidable repository of sparse tensors and associated tools, namely, the FROSTT database [39]. For this purpose, we selected two large and sparse tensors, whose salient characteristics are presented in Table 5. The first tensor, NELL-2 [9], is a dataset that is commonly employed in machine learning systems for establishing relationships among various entities. It is a three-dimensional dataset, where the modes correspond to entity, relation, and entity, respectively. The second tensor, the NIPS Publications dataset [25], was collected by Globerson *et al.* and contains papers published in NIPS between 1987 and 2003. The tensor has four modes that correspond to paper, author, word, and year, respectively. The entries of the tensor denote the frequency of the occurrence of words in each paper.

Table 6: Relative error and running time of both HOID and R-HOID on the tensors defined in Table 5. We set the target multirank of $(20, 20, 50)$ and $(\hat{r}_1, \hat{r}_2, \hat{r}_3) = (15, 15, 30)$ for the NELL-2, while a multirank of $(50, 50, 50)$ and $(\hat{r}_1, \hat{r}_2, \hat{r}_3) = (25, 25, 25)$ for the NIPS and an oversampling parameter of $p = 5$ as inputs.

Method		HOID-DEIM	HOID-LDEIM	R-HOID-DEIM	R-HOID-LDEIM
NELL-2	Err	0.086911	0.10288	0.090825	0.10776
	CPU	95.989	59.590	7.1387	4.8956
NIPS	Err	0.50393	0.66685	0.56733	0.70049
	CPU	175.83	96.301	10.297	6.1198

Table 5: Summary of sparse tensor examples from the FROSTT database-we include the details for both the full datasets and the condensed datasets used in our experiments.

Original tensor	Order	Size	Nonzeros
NELL-2	3	$12092 \times 9184 \times 28818$	76,879,419
NIPS	4	$2482 \times 2862 \times 14036 \times 17$	3,101,609
Condensed tensor	Order	Size	Nonzeros
NELL-2	3	$532 \times 682 \times 606$	7069
NIPS	3	$632 \times 647 \times 684$	4561

First, we ran both the HOID and R-HOID algorithms on the NELL-2 and NIPS defined in Table 5, which produce a multirank- $(20, 20, 50)$ and a multirank- $(50, 50, 50)$ approximation respectively. As inputs to our test algorithms, we use the parameter of the L-DEIM $(\hat{r}_1, \hat{r}_2, \hat{r}_3) = (15, 15, 30)$ for the NELL-2 and use $(\hat{r}_1, \hat{r}_2, \hat{r}_3) = (25, 25, 25)$ for the NIPS, and the oversampling parameter $p = 5$. Then we ran the Hybrid and the R-Hybrid algorithm on the NELL 2 and NIPS, where we keep the same parameters and the target multirank and we preserve the first two modes of the original tensors. The corresponding results are displayed in Tables 6 and 7, where we can see that the randomized algorithms give comparable relative errors at substantially less cost.

Table 7: Relative error and running time of Hybrid, R-Hybrid-PQR, R-Hybrid-DEIM and R-Hybrid-LDEIM on the tensors defined in Table 5. The parameters and target multirank are the same as in Table 6 and we preserve the first two modes of the original tensors.

Method		Hybrid	R-hybrid-PQR	R-hybrid-DEIM	R-hybrid-LDEIM
NELL-2	Err	0.086615	0.090311	0.088822	0.11510
	CPU	118.59	8.4060	9.7856	8.7567
NIPS	Err	0.43845	0.50652	0.49945	0.65049
	CPU	157.99	15.505	19.600	12.747

7 Conclusion

In this paper, by combining the random sampling techniques with the L-DEIM method, we develop new efficient randomized algorithms for computing the approximate CUR-type and hybrid CUR decomposition for tensors in the Tucker format with a given target multilinear rank. We also provided the detailed probabilistic analysis for the proposed randomized algorithms. Theoretical analysis and numerical examples illustrate that exploiting the randomized techniques results in a big improvement in terms of the CPU time while keeping a high degree of accuracy. Finally, it is natural to consider applying the L-DEIM for developing randomized algorithms that adaptively find a low

multirank representation satisfying a given tolerance, which is particularly useful when the target rank is not known in advance, and it will be discussed in our future work.

Acknowledgments

This work is supported by the National Natural Science Foundation of China (No. 12271108 and 11801534), the Innovation Program of Shanghai Municipal Education Committee and the Fundamental Research Funds for the Central Universities (No. 202264006).

References

- [1] S. AHMADI-ASL, S. ABUKHOVICH, M. G. ASANTE-MENSAH, A. CICHOCKI, A. H. PHAN, T. TANAKA, AND I. OSELEDETS, *Randomized algorithms for computation of Tucker decomposition and higher order SVD (HOSVD)*, IEEE Access, 9 (2021), pp. 28684–28706.
- [2] S. AHMADI-ASL, C. F. CAIAFA, A. CICHOCKI, A. H. PHAN, T. TANAKA, I. OSELEDETS, AND J. WANG, *Cross tensor approximation methods for compression and dimensionality reduction*, IEEE Access, 9 (2021), pp. 150809–150838.
- [3] AT&T LABORATORIES AT CAMBRIDGE, *Olivetti database of faces*. <https://cs.nyu.edu/~roweis/data.html>, 2002.
- [4] B. W. BADER AND T. G. KOLDA, *Efficient MATLAB computations with sparse and factored tensors*, SIAM Journal on Scientific Computing, 30 (2008), pp. 205–231.
- [5] M. BARRAULT, Y. MADAY, N. C. NGUYEN, AND A. T. PATERA, *An ‘empirical interpolation’ method: application to efficient reduced-basis discretization of partial differential equations*, Comptes Rendus Mathematique, 339 (2004), pp. 667–672.
- [6] E. BEGOVIĆ KOVAČ, *Hybrid CUR-type decomposition of tensors in the Tucker format*, BIT Numerical Mathematics, 62 (2022), pp. 125–138.
- [7] H. CAI, K. HAMM, L. HUANG, AND D. NEEDELL, *Mode-wise tensor decompositions: Multi-dimensional generalizations of CUR decompositions*, Journal of Machine Learning Research, 22 (2021), pp. 1–36.
- [8] J. D. CARROLL AND J.-J. CHANG, *Analysis of individual differences in multidimensional scaling via an N-way generalization of “Eckart-Young” decomposition*, Psychometrika, 35 (1970), pp. 283–319.
- [9] S. CHATURANTABUT AND D. C. SORENSSEN, *Nonlinear model reduction via discrete empirical interpolation*, SIAM Journal on Scientific Computing, 32 (2010), pp. 2737–2764.
- [10] M. CHE, J. CHEN, AND Y. WEI, *Perturbations of the TCUR decomposition for tensor valued data in the Tucker format*, Journal of Optimization Theory and Applications, 194 (2022), pp. 852–877.
- [11] M. CHE AND Y. WEI, *Randomized algorithms for the approximations of Tucker and the tensor train decompositions*, Advances in Computational Mathematics, 45 (2019), pp. 395–428.
- [12] M. CHE AND Y. WEI, *Randomized algorithms*, in Theory and Computation of Complex Tensors and its Applications, Springer, 2020, pp. 215–246.

- [13] M. CHE, Y. WEI, AND H. YAN, *The computation of low multilinear rank approximations of tensors via power scheme and random projection*, SIAM Journal on Matrix Analysis and Applications, 41 (2020), pp. 605–636.
- [14] M. CHE, Y. WEI, AND H. YAN, *An efficient randomized algorithm for computing the approximate Tucker decomposition*, Journal of Scientific Computing, 88 (2021), pp. 1–29.
- [15] M. CHE, Y. WEI, AND H. YAN, *Randomized algorithms for the low multilinear rank approximations of tensors*, Journal of Computational and Applied Mathematics, 390 (2021), p. 113380.
- [16] J. CHEN, Y. WEI, AND Y. XU, *Tensor CUR decomposition under t-product and its perturbation*, Numerical Functional Analysis and Optimization, (2022), pp. 1–25.
- [17] H. CHENG, Z. GIMBUTAS, P.-G. MARTINSSON, AND V. ROKHLIN, *On the compression of low rank matrices*, SIAM Journal on Scientific Computing, 26 (2005), pp. 1389–1404.
- [18] A. CORTINOVIS AND D. KRESSNER, *Low-rank approximation in the Frobenius norm by column and row subset selection*, SIAM Journal on Matrix Analysis and Applications, 41 (2020), pp. 1651–1673.
- [19] L. DE LATHAUWER, B. DE MOOR, AND J. VANDEWALLE, *A multilinear singular value decomposition*, SIAM Journal on Matrix Analysis and Applications, 21 (2000), pp. 1253–1278.
- [20] P. DRINEAS AND M. W. MAHONEY, *A randomized algorithm for a tensor-based generalization of the singular value decomposition*, Linear Algebra and its Applications, 420 (2007), pp. 553–571.
- [21] P. DRINEAS, M. W. MAHONEY, AND S. MUTHUKRISHNAN, *Relative-error CUR matrix decompositions*, SIAM Journal on Matrix Analysis and Applications, 30 (2008), pp. 844–881.
- [22] Z. DRMAC AND S. GUGERCIN, *A new selection operator for the discrete empirical interpolation method—improved a priori error bound and extensions*, SIAM Journal on Scientific Computing, 38 (2016), pp. A631–A648.
- [23] P. Y. GIDISU AND M. E. HOCHSTENBACH, *A hybrid DEIM and leverage scores based method for CUR index selection*, Progress in Industrial Mathematics at ECMI 2021, (2022), pp. 147–153.
- [24] P. Y. GIDISU AND M. E. HOCHSTENBACH, *A Restricted SVD type CUR decomposition for matrix triplets*, arXiv:2204.02113, (2022).
- [25] A. GLOBERSON, G. CHECHIK, F. PEREIRA, AND N. TISHBY, *Euclidean Embedding of Co-occurrence Data*, The Journal of Machine Learning Research, 8 (2007), pp. 2265–2295.
- [26] M. GU AND S. C. EISENSTAT, *Efficient algorithms for computing a strong rank-revealing QR factorization*, SIAM Journal on Scientific Computing, 17 (1996), pp. 848–869.
- [27] N. HALKO, P.-G. MARTINSSON, AND J. A. TROPP, *Finding structure with randomness: Probabilistic algorithms for constructing approximate matrix decompositions*, SIAM Review, 53 (2011), pp. 217–288.
- [28] K. HAMM AND L. HUANG, *Perturbations of CUR decompositions*, SIAM Journal on Matrix Analysis and Applications, 42 (2021), pp. 351–375.
- [29] E. P. HENDRYX, B. M. RIVIÈRE, AND C. G. RUSIN, *An extended DEIM algorithm for subset selection and class identification*, Machine Learning, 110 (2021), pp. 621–650.
- [30] I. T. JOLLIFFE, *Discarding variables in a principal component analysis. i: Artificial data*, Journal of the Royal Statistical Society: Series C (Applied Statistics), 21 (1972), pp. 160–173.

- [31] M. E. KILMER, K. BRAMAN, N. HAO, AND R. C. HOOVER, *Third-order tensors as operators on matrices: A theoretical and computational framework with applications in imaging*, SIAM Journal on Matrix Analysis and Applications, 34 (2013), pp. 148–172.
- [32] T. G. KOLDA AND B. W. BADER, *Tensor decompositions and applications*, SIAM Review, 51 (2009), pp. 455–500.
- [33] M. W. MAHONEY, M. MAGGIONI, AND P. DRINEAS, *Tensor-CUR decompositions for tensor-based data*, SIAM Journal on Matrix Analysis and Applications, 30 (2008), pp. 957–987.
- [34] P.-G. MARTINSSON, V. ROKHLIN, AND M. TYGERT, *A randomized algorithm for the decomposition of matrices*, Applied and Computational Harmonic Analysis, 30 (2011), pp. 47–68.
- [35] R. MINSTER, A. K. SAIBABA, AND M. E. KILMER, *Randomized algorithms for low-rank tensor decompositions in the Tucker format*, SIAM Journal on Mathematics of Data Science, 2 (2020), pp. 189–215.
- [36] L. QI, Y. CHEN, M. BAKSHI, AND X. ZHANG, *Triple decomposition and tensor recovery of third order tensors*, SIAM Journal on Matrix Analysis and Applications, 42 (2021), pp. 299–329.
- [37] A. K. SAIBABA, *HOID: higher order interpolatory decomposition for tensors based on Tucker representation*, SIAM Journal on Matrix Analysis and Applications, 37 (2016), pp. 1223–1249.
- [38] B. SAVAS AND L. ELDÉN, *Handwritten digit classification using higher order singular value decomposition*, Pattern Recognition, 40 (2007), pp. 993–1003.
- [39] S. SMITH, J. W. CHOI, J. LI, R. VUDUC, J. PARK, X. LIU, AND G. KARYPIS, *FROSTT: The formidable repository of open sparse tensors and tools*, <http://frostdt.io>, 2017.
- [40] D. C. SORENSEN AND M. EMBREE, *A DEIM induced CUR factorization*, SIAM Journal on Scientific Computing, 38 (2016), pp. A1454–A1482.
- [41] D. B. SZYLD, *The many proofs of an identity on the norm of oblique projections*, Numerical Algorithms, 42 (2006), pp. 309–323.
- [42] L. R. TUCKER, *Some mathematical notes on three-mode factor analysis*, Psychometrika, 31 (1966), pp. 279–311.
- [43] E. TYRTYSHNIKOV, *Incomplete cross approximation in the mosaic-skeleton method*, Computing, 64 (2000), pp. 367–380.
- [44] Y. WEI, P. STANIMIROVIĆ, AND M. PETKOVIĆ, *Numerical and Symbolic Computations of Generalized Inverses*, Hackensack, NJ: World Scientific, 2018.